First demonstration of positive allosteric–like modulation at the human wild type translocator protein (TSPO)

Rajeshwar Narlawar [1]*, Eryn L. Werry[2]*, Alana M. Scarf[3], Raphy Hanani[1], Sook Wern Chua[4], Victoria A. King[3], Melissa L. Barron[2], Ralph N. Martins[5], Lars M. Ittner[4], Louis M. Rendina[1] and Michael Kassiou[1,2#]

*Joint first author

#Corresponding author
Tel: +612 9351 2745
michael.kassiou@sydney.edu.au

[1] School of Chemistry, The University of Sydney, NSW 2006 Australia

[2] Faculty of Health Sciences, The University of Sydney, NSW 2006 Australia

[3] School of Medical Sciences (Pharmacology), Bosch Institute, The University of Sydney, NSW 2006 Australia

[4] Dementia Research Unit, School of Medical Sciences, University of New South Wales, NSW 2052 Australia.

[5] School of Medical Sciences, Edith Cowan University, WA 6050 Australia.

Abstract

We show that changing the number and position of nitrogen atoms in the heteroatomic core of a pyrazolopyrimidine acetamide is sufficient to induce complex binding to wild type human TSPO. Only compounds with this complex binding profile lacked intrinsic effect on glioblastoma proliferation but positively modulated the anti–proliferative effects of a synthetic TSPO ligand. To the best of our knowledge this is the first demonstration of allosteric–like interaction at the wild type human TSPO.

Graphical abstract

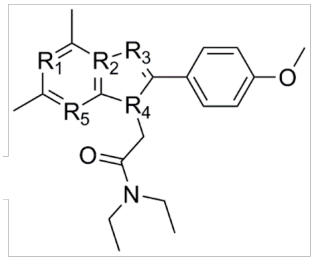

1 R_1=C, R_2=C, R_3=C, R_4=N, R_5=C
2 R_1=C, R_2=C, R_3=N, R_4=N, R_5=C
3 R_1=C, R_2=C, R_3=N, R_4=N, R_5=N
4 R_1=C, R_2=N, R_3=N, R_4=C, R_5=N
5 R_1=N, R_2=C, R_3=N, R_4=N, R_5=N

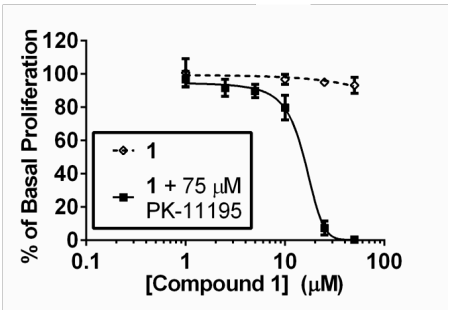

Introduction

The 18 kDa translocator protein (TSPO) is a highly–conserved five transmembrane protein most commonly found in the outer mitochondrial membrane.[1] It is suggested to be a part of the mitochondrial permeability transition pore (MPTP) in a complex with the voltage–dependant anion carrier (VDAC) and the adenine nucleotide transporter (ANT).[2, 3] TSPO is expressed at highest levels in steroidogenic cells.[1] Baseline TSPO expression levels in the brain are low, but TSPO are upregulated in reactive glia in areas damaged by neurodegenerative diseases, and also in cancers such as glioma.[4-8] Conversely, TSPO expression is downregulated in lymphocytes and leukocytes in a number of anxiety disorders.[8] As such, TSPO has become a target for development of drug treatments and diagnostic imaging agents for use in cancer, neurodegenerative diseases and anxiety.[4-6, 8, 9]

Development of these drugs, however, has been hindered by the emerging complexity of ligand interactions at the TSPO. Several classes of ligands interact with the TSPO at distinct binding sites. The endogenous ligand cholesterol binds to an area of the cytosolic C–terminus defined as the cholesterol recognition amino acid consensus (CRAAC) domain.[10] Other endogenous ligands such as protoporphyrin IX along with many synthetic ligands, bind to loop 1 of the N–terminal. Site–directed mutagenesis, however, suggests residues in this loop important for binding of the prototypic benzodiazepine Ro 5–4864 are not critical for binding of the first–generation synthetic isoquinoline carboxamide ligand PK 11195.[11]

Another well–documented influence on binding complexity to the human TSPO is the rs6971 polymorphism. This polymorphism located in exon 4 of the TSPO gene results in the substitution of alanine with threonine at amino acid residue 147.[12] Homozygous expression of Ala147 TSPO in human brain tissue and leukocytes results in high affinity binding, while homozygous expression of Thr147 TSPO results in low affinity binding and heterozygous expression results in complex two–site mixed affinity binding.[13, 14] This modulation of binding has functional outcomes with Ala147 homozygous leukocytes producing more pregnenalone than homozygous Thr147 and heterozygous leukocytes.[12] A phase II clinical trial of the TSPO ligand XBD173 in generalized anxiety disorder failed, partly due to the presence of this polymorphism in subjects (ClinicalTrials.gov NCT00108836).

Given the already documented complex nature of binding to the TSPO, and that multiple drug binding sites exist on the TSPO, it may be possible that allosteric–like interactions occur at the TSPO. In fact in rat brain cortical synaptosomes, a multi–phasic Scatchard analysis of radioligand binding results suggested complex, possibly allosteric, interactions between the synthetic steroid stanozolol and PK 11195,[15] however, interpretation of binding nature from Scatchard plots can be ambiguous, and this study did not characterize whether stanozolol altered the potency of PK 11195. Furthermore it was not documented whether the TSPO in this study had the Ala147Thr polymorphism, and hence whether the results could have been explained solely by the presence of the polymorphism. As such, the extent to which complex allosteric–like interactions occur at the human Ala147 (wild type) TSPO is currently unclear.

Pyrazolo [1,5–*a*] pyrimidine acetamides are a promising class of TSPO ligands with recent in vitro and human imaging studies suggesting derivatives of this class have a high affinity, good

bioavailability and are well–tolerated.[2, 16] However, the number of nitrogen atoms in the central heteroatomic core of TSPO ligands can impact TSPO binding affinity.[17] In the present study, we aimed to examine how complexity in binding to human Ala147 (wild type) TSPO is affected by changing the number and position of nitrogen atoms in the central heteroatomic core of a pyrazolopyrimidine acetamide (**4**). We show that changing the number and position of nitrogen atoms is sufficient to induce complex binding to Ala147 human TSPO. For the first time, we show that only compounds with this complex binding profile have no effect on glioblastoma proliferation by themselves but positively modulate the anti–proliferative effects of PK 11195 in an allosteric–like manner.

Results:

Chemistry

A set of TSPO ligands were designed by changing the number and position of the nitrogen atoms in the hetero–bicyclic core of **4,** resulting in various heterocylic derivatives such as the indole **1**, benzimidazole **2**, imidazopyridine **3** and purine **5** derivatives (Table 1). The synthesis of these novel derivatives began with the indole **1** as outlined in **Scheme 1**. Briefly, 3,5–dimethyl phenyl hydrazine **7** was synthesized from commercially available 3,5–dimethyl aniline **6**. Diazotization of aniline **6** using $NaNO_2$ in HCl, followed by the reaction with $SnCl_2$ in HCl, gave the hydrazine hydrochloride as colorless solid. Phenyl hydrazine hydrochlride was then treated with 3 M KOH to afford the free phenyl hydrazine which then underwent the Fischer indole synthesis. Phenyl hydrazine **7**, 4–methoxy acetophenone **8** and catalytic acetic acid were refluxed in absolute ethanol to afford the phenylhydrazone as a golden-coloured solid. Crude hydrazone and polyphosphoric acid mixture was heated at 120°C to afford the indole **9** in moderate yield. *N*–

alkylation of indole **9** was achieved using 2–chloro–*N*,*N*–diethylacetamide and NaH in DMF to afford the desired indole acetamide **1**.

The bezimidazole derivative **2** was synthesized as outlined in **Scheme 2**. Commercially available 2,4–dimethyl aniline **10** was nitrated using a documented procedure.[18] The nitro group of **11** was reduced using Zn powder and hydrazine hydrate in *n*–butanol at reflux to afford the diamine **12** in good yield. 2–(4–(benzyloxy)phenyl)–4,6–dimethyl–1*H*–benzo[*d*]imidazole **14** was synthesized in one step from 3,5–dimethylbenzene–1,2–diamine **12** and 4–benzyloxybenzaldehyde **13**, in the presence of ammonium acetate under microwave conditions. *N*–alkylation of benzimidazole **14** proceeded in good yield in the presence of sodium hydride and chloro–*N*,*N*–diethylacetamide to give **15**. The benzyl group of **15** was deprotected under hydrogenolysis using 10 % Pd/C in methanol to afford the phenol **16**. The phenol **16** was alkylated using sodium hydride and methyl iodide to give the corresponding desired aryl ether **2**.

The imidazopyridine derivative **3** was synthesized as outlined in **Scheme 3**. Commercially available 2–amino–4, 6–dimethylpyridine **17** was regioselectively brominated at the doubly activated 5–position and upon treatment with 0.5 equivalents of 1,3– dibromohydantoin at –50 °C to afforded **18**. Installation of the bromine at the 5–position was essential for directing the subsequent nitration at 3–position. Under standard nitration conditions the nitro pyridine derivative **19** was obtained in good yield. The nitro compound **19** was then successfully converted into the corresponding diamine **20** in 90% yield using a combination of zinc and hydrazine monohydrate. The product was sufficiently pure and was used in the next step without further purification. Diamine **20** was cyclized under microwave irradiation and in the presence of

ammonium acetate and 4–methoxy benzaldehyde to give imidazopyridine **21**. *N*–alkylation of **21** was achieved using sodium hydride and chloro–*N*, *N*–diethylacetamide resulting in **22**. Finally, the debromination of **22** was carried out using *n*–BuLi in THF at –50 °C to afford desired imidazopyridine derivative **3** in good yield.

The pyrazolopyrimidine derivative **4** was synthesized following a published procedure[19] and was considered to be of >95 % purity according to ^{1}H and ^{13}C NMR spectroscopy and elemental analysis.

The purine derivative **5** was synthesized in three steps as depicted in **Scheme 4**. The synthesis of the purine derivative began with *N*–alkylation of commercially available 2,6– dichloro–9*H*–purine **23**. *N*–alkylation was performed using sodium hydride and chloro–*N*,*N*–diethylacetamide which resulted in an inseparable mixture of two products believed to be regioisomers of **24**. Thus, the subsequent cross–coupling reaction was performed using the mixture. The crude regioisomeric mixture was utilized in a palladium–catalyzed methylation in the presence of trimethylaluminium. tetrakis(triphenyphosphine)palladium(0). 2– (2,6–Dimethyl–9*H*–purin–9–yl) –*N*,*N*–diethylacetamide **25** was isolated in pure form at this stage and in moderate yield (45% over 2 steps). Direct C–2 arylation was employed using 4–iodo anisole, $Pd(OAc)_2$, CuI and Cs_2CO_3 to obtain the desired purine derivative **5** in moderate yield.

Sequencing for rs6971

Sequencing was carried out on HEK 293T and T98G cells to establish the nature of their genetic sequence at the 439th nucleotide in the human TSPO gene. Both cell lines expressed a guanine at this position in the gene, indicating they both have alanine as their 147th TSPO amino acid and hence do not have the rs6971 polymorphism.

Binding interactions

The TSPO binding nature of compounds **1–5** was determined by competition radioligand binding against [^{3}H]PK 11195 in HEK 293T and T98G cell membranes. Results are displayed in Table 1 and Figure 1. In general, compounds with 3 nitrogen atoms in the heterocyclic core (**3, 4**) interacted with the TSPO in a one–site manner with a hill slope of 1 at the same site as [^{3}H]PK 11195, while compounds with less than 3 nitrogen atoms displayed complex hill slopes. Compound **1** had a hill slope more negative than –1 at HEK 293T and T98G membranes ($p<0.05$), while **2** had a hill slope more positive than –1 at T98G membranes ($p<0.05$). A binding model could not be fitted for compound **5** as it did not bind to the TSPO, even up to 10 μM.

In HEK 293T cells, all assessed compounds displayed TSPO binding affinity in the low nM range apart from the non–binding purine derivative (**5**). All compounds except the pyrazolopyrimidine acetamide (**4**) showed a lowering of affinity to TSPO in T98G cells, particularly the indole (**1**). Excluding compound **5**, affinity order in T98G cells followed the number of nitrogen atoms present in the heterocyclic core, with compounds containing 3

nitrogen atoms showing the highest affinity (**4** followed by **3**), and the compound with one nitrogen atom in the heterocyclic core showing lowest affinity (**1**).

Effects on T98G proliferation and viability

A number of TSPO ligands, including PK 11195, have shown anti–proliferative effects on glioma cell lines.[6] We examined whether our novel compounds affected proliferation of the human glioma cell line T98G, and whether they enhanced the anti–proliferative effect of PK 11195. Compounds **1**–**5** did not affect the basal proliferation of T98G cells (1–100 μM). Although it did not have an anti–proliferative effect by itself, **1** significantly increased the anti–proliferative effect of an ~EC_{10} concentration of PK 11195 at 10 μM and higher ($p<0.05$; Figure 2). The EC_{50} for this potentiating effect was 14.73 ± 1.1 μM. Similarly, although **2** did not have an anti–proliferative effect by itself, it significantly increased the anti–proliferative effect of an ~EC_{10} concentration of PK 11195 at 62.5 μM ($p<0.05$; Figure 2). Up to 100 μM, compounds **3**, **4** and **5** did not significantly modulate the anti–proliferative effect of an ~EC_{10} concentration of PK 11195 (Supplementary Table 1).

Cell viability was not significantly affected by compounds **1**–**5** in the absence, or presence, of an ~EC_{10} concentration of PK 11195.

Discussion and Conclusions

In this study, we aimed to explore the impact on complexity of TSPO interaction by altering the heterocyclic core of a high affinity pyrazolopyrimidine acetamide (**4**). Initially we examined the

impact of nitrogen atom position on TSPO interaction by comparing the affinity and efficacy of the lead pyrazolopyrimidine **4** and the imidazopyridine–derivative **3**. Template hopping of **4** leading to the imidazalopyridine–derivative **3** decreased TSPO affinity, however both compounds showed normal one–site binding, and these compounds did not modulate PK 11195 anti–proliferative effects.

We then explored the impact of changing the number of nitrogen atoms in the heterocyclic core on TSPO interaction. Increasing the number of nitrogen atoms to make the purine derivative **1** removed the ability of the compound to bind to TSPO, suggesting the number of nitrogen atoms in the heterocyclic core is critical for affinity. This in agreement with a previous study whereby *N,N*–dialkyl–4–phenylquinazoline–2–carboxamides demonstrated improved TSPO affinity over *N,N*–dialkyl (2–phenylindol–3–yl)glyoxylamides.[17]

Given this sensitivity to TSPO affinity found by increasing the number of nitrogen atoms in the heterocyclic core, we examined the impact of decreasing the number of nitrogen atoms on TSPO interaction by screening an indole– and a benzimidazole–derivative. The indole–derivative **1** showed a hill slope more negative than –1 in competition with the synthetic TSPO ligand [^{3}H]PK 11195. In classical receptor pharmacology, a hill slope of –1 indicates binding interactions that obey the law of mass action, while a hill slope more negative than –1 suggests positive co–operativity, where the binding of the novel compound at one site enhances the affinity of the radiolabelled compound at another site.[20] One way that this may manifest functionally is in positive allosteric modulation, where a ligand may have no intrinsic efficacy but may enhance the functional effect of a second ligand.[21] Through assays indexing anti–proliferative potential of these novel compounds we showed that the indole–derivative did not affect proliferation by

itself, but rather it enhanced PK 11195's anti–proliferative affects. Given that this complexity of interaction occurred in the verified absence of the rs6791 polymorphism, which is the most well–documented cause of affinity and potency change at the TSPO, it is possible that this complex interaction is allosteric–like behavior.

It is unclear, however, the extent to which the observed behavior of the indole–derivative can be termed 'classical' allosterism. Allosterism is most widely characterized in receptors, ion channels and enzymes and the TSPO does not fit within these classes, so it is unknown as to the extent it obeys normal pharmacological interactions seen in these more widely studied protein categories. Further, a classic allosteric modulator enhances the potency of an orthosteric ligand, that is, a ligand that binds to the same site as an endogenous ligand. PK 11195 is not an endogenous ligand and may bind at different sites to the endogenous TSPO ligands cholesterol and protoporphyrin IX.[22, 23] Whether the indole–derivate binds to the orthosteric TSPO sites to facilitate the effects of PK 11195[11] is an important question to resolve. Furthermore, whether the indole–derivative also facilitates the effects of the endogenous TSPO ligands, hence showing more classical allosteric behavior, remains to be examined.

The benzimidazole–derivative **2** also enhanced PK 11195 anti–proliferative affects without inducing anti–proliferative effects on its own. The benzimidazole also had a hill slope that deviated from –1 in competition radioligand binding studies with [3H]PK 11195, but unexpectedly the hill slope was more shallow than –1. In classical receptor pharmacology, this would predict negative modulation of PK 11195,[20] the opposite to the functional effects observed in this study. As discussed above, this may suggest that the TSPO does not operate within classical definitions of co–operativity and allosteric receptor pharmacology. There are, however,

two alternative explanations A hill slope more shallow than –1 in competition radioligand binding may also suggest that the binding occurs at heterogeneous receptors that may bind the ligand with different affinities.[20] TSPO is known to exist in several forms – as a monomer, dimer and polymer.[24, 25] Recent structural resolution of a bacterial analogue of TSPO led to predictions that potential dimerization of the TSPO from monomeric form could bring separated binding sites into closer proximity, creating the potential for co–operative interactions,[23] suggesting the monomeric, dimeric and polymeric forms of TSPO could be thought of as heterogenous receptors. In support of this prediction, human chorionic gonadotropin can increase binding of PK 11195 to TSPO in mouse MA–10 Leydig testicular tumor cells in a manner than temporally correlates with its ability to induce rapid polymerization of TSPO.[26, 27] It is important, then, to examine the effect of the benzimidazole **2** on the equilibrium between monomeric, dimeric and polymeric forms of the TSPO in T98G cells to determine if the positive modulation could be due to disruption of this equilibrium.

A second explanation for the shallow hill slope induced by the benzimidazole **2** could relate to the existence of TSPO in a complex with VDAC and ANT. A shallow hill slope can be seen when insufficient accessory proteins are available to associate with a protein that usually exists in a complex[20]. TSPO is predominantly found in the mitochondria[1] where there is ample VDAC and ANT, but can translocate to the nucleus in some cancers.[28] It may be that in cancer cells, nuclear and cytoplasmic TSPO don't have enough VDAC and ANT for adequate complex formation. This may explain why a shallow hill slope was only induced by the benzimidazole **2** on binding to TSPO from glioma cells and not from the mitochondria of HEK cells.

Considering neither compound with three nitrogens in the heterocyclic core showed allosteric–like behavior, and the indolic derivative **1** had more pronounced positive modulation than the benzimidazole **2**, these results suggest a lower number of nitrogen atoms in the heteroatomic core is likely the key to inducing allosteric–like effects of pyrazolopyrimidine acetamide–derivatives. We plan to further explore this by examining the allosteric potential of isoindole and indazole derivatives.

In conclusion, we have identified an indole **1** and benzimidazole derivative **2** of pyrazolopyrimidine acetamide **4** which show complex binding, lack of intrinsic activity and positive modulation of the anti–proliferative effects of PK 11195. To the best of our knowledge, this is the first demonstration of allosteric–like behavior at the wild-type human TSPO. Although the mechanisms behind this potentiation are as yet undefined, identification of such compounds may open the way for development of novel allosteric–like anxiolytics, neuroprotective agents and anti–cancer drugs that target the TSPO.

Experimental section:

Chemistry:

All compounds synthesized as per the Results and SI sections were analysed by ^{1}H and ^{13}C NMR and high-resolution electrospray ionization mass spectroscopy. Full experimental procedures and results of analyses can be found in the Supplementary Information.

Acknowledgements

The authors wish to acknowledge the support received from the Bosch Institute Molecular Biology Facility, and the expert help of facility staff, especially Dr Donna Lai and Dr Sheng Hua. Work performed at The University of Sydney and presented herein was supported in part by the European Union's Seventh Framework Programme [FP7/2007-2013] INMiND (Grant agreement No. HEALTH-F2-2011-278850).

Abbreviations Used

ANT	adenine nucleotide transporter
CRAAC	cholesterol recognition amino acid consensus
HEK	human embryonic kidney
MPTP	mitochondrial permeability transition pore
TSPO	translocator protein
VDAC	voltage–dependant anion carrier

Supplementary Information

Synthetic procedure and spectral data of compounds, Biological procedures, Supplementary Table 1

References and notes:

(1) Papadopoulos, V.; Baraldi, M.; Guilarte, T. R.; Knudsen, T. B.; Lacapere, J. J.; Lindemann, P.; Norenberg, M. D.; Nutt, D.; Weizman, A.; Zhang, M. R.; Gavish, M. Translocator protein (18kDa): new nomenclature for the peripheral-type benzodiazepine receptor based on its structure and molecular function. *Trends Pharmacol Sci* **2006,** 27, 402-9.

(2) Scarf, A. M.; Ittner, L. M.; Kassiou, M. The translocator protein (18 kDa): central nervous system disease and drug design. *J Med Chem* **2009,** 52, 581-92.

(3) McEnery, M. W.; Snowman, A. M.; Trifiletti, R. R.; Snyder, S. H. Isolation of the mitochondrial benzodiazepine receptor: association with the voltage-dependent anion channel and the adenine nucleotide carrier. *Proc Natl Acad Sci U S A* **1992,** 89, 3170-4.

(4) Politis, M.; Su, P.; Piccini, P. Imaging of microglia in patients with neurodegenerative disorders. *Front Pharmacol* **2012,** 3, 96.

(5) Chua, S. W.; Kassiou, M.; Ittner, L. M. The translocator protein as a drug target in Alzheimer's disease. *Expert Rev Neurother* **2014,** 14, 439-48.

(6) Austin, C. J.; Kahlert, J.; Kassiou, M.; Rendina, L. M. The translocator protein (TSPO): a novel target for cancer chemotherapy. *Int J Biochem Cell Biol* **2013,** 45, 1212-6.

(7) Lacapere, J. J.; Papadopoulos, V. Peripheral-type benzodiazepine receptor: structure and function of a cholesterol-binding protein in steroid and bile acid biosynthesis. *Steroids* **2003,** 68, 569-85.

(8) Rupprecht, R.; Papadopoulos, V.; Rammes, G.; Baghai, T. C.; Fan, J.; Akula, N.; Groyer, G.; Adams, D.; Schumacher, M. Translocator protein (18 kDa) (TSPO) as a therapeutic target for neurological and psychiatric disorders. *Nat Rev Drug Discov* **2010,** 9, 971-88.

(9) Rupprecht, R.; Rammes, G.; Eser, D.; Baghai, T. C.; Schule, C.; Nothdurfter, C.; Troxler, T.; Gentsch, C.; Kalkman, H. O.; Chaperon, F.; Uzunov, V.; McAllister, K. H.; Bertaina-Anglade, V.; La Rochelle, C. D.; Tuerck, D.; Floesser, A.; Kiese, B.; Schumacher, M.; Landgraf, R.; Holsboer, F.; Kucher, K. Translocator protein (18 kD) as target for anxiolytics without benzodiazepine-like side effects. *Science* **2009,** 325, 490-3.

(10) Li, H.; Papadopoulos, V. Peripheral-type benzodiazepine receptor function in cholesterol transport. Identification of a putative cholesterol recognition/interaction amino acid sequence and consensus pattern. *Endocrinology* **1998,** 139, 4991-7.

(11) Farges, R.; Joseph-Liauzun, E.; Shire, D.; Caput, D.; Le Fur, G.; Ferrara, P. Site-directed mutagenesis of the peripheral benzodiazepine receptor: identification of amino acids implicated in the binding site of Ro5-4864. *Mol Pharmacol* **1994,** 46, 1160-7.

(12) Costa, B.; Pini, S.; Gabelloni, P.; Da Pozzo, E.; Abelli, M.; Lari, L.; Preve, M.; Lucacchini, A.; Cassano, G. B.; Martini, C. The spontaneous Ala147Thr amino acid substitution within the translocator protein influences pregnenolone production in lymphomonocytes of healthy individuals. *Endocrinology* **2009,** 150, 5438-45.

(13) Kreisl, W. C.; Jenko, K. J.; Hines, C. S.; Lyoo, C. H.; Corona, W.; Morse, C. L.; Zoghbi, S. S.; Hyde, T.; Kleinman, J. E.; Pike, V. W.; McMahon, F. J.; Innis, R. B.; Biomarkers Consortium, P. E. T. R. P. T. A genetic polymorphism for translocator protein 18 kDa affects both in vitro and in vivo radioligand binding in human brain to this putative biomarker of neuroinflammation. *J Cereb Blood Flow Metab* **2013,** 33, 53-8.

(14) Owen, D. R.; Yeo, A. J.; Gunn, R. N.; Song, K.; Wadsworth, G.; Lewis, A.; Rhodes, C.; Pulford, D. J.; Bennacef, I.; Parker, C. A.; StJean, P. L.; Cardon, L. R.; Mooser, V. E.; Matthews, P. M.; Rabiner, E. A.; Rubio, J. P. An 18-kDa translocator protein (TSPO) polymorphism explains differences in binding affinity of the PET radioligand PBR28. *J Cereb Blood Flow Metab* **2012,** 32, 1-5.

(15) Masonis, A. E.; McCarthy, M. P. Direct interactions of androgenic/anabolic steroids with the peripheral benzodiazepine receptor in rat brain: implications for the psychological and physiological manifestations of androgenic/anabolic steroid abuse. *J Steroid Biochem Mol Biol* **1996,** 58, 551-5.

(16) Corcia, P.; Tauber, C.; Vercoullie, J.; Arlicot, N.; Prunier, C.; Praline, J.; Nicolas, G.; Venel, Y.; Hommet, C.; Baulieu, J. L.; Cottier, J. P.; Roussel, C.; Kassiou, M.; Guilloteau, D.; Ribeiro, M. J. Molecular imaging of microglial activation in amyotrophic lateral sclerosis. *PLoS One* **2012,** 7, e52941.
(17) Castellano, S.; Taliani, S.; Viviano, M.; Milite, C.; Da Pozzo, E.; Costa, B.; Barresi, E.; Bruno, A.; Cosconati, S.; Marinelli, L.; Greco, G.; Novellino, E.; Sbardella, G.; Da Settimo, F.; Martini, C. Structure-activity relationship refinement and further assessment of 4-phenylquinazoline-2-carboxamide translocator protein ligands as antiproliferative agents in human glioblastoma tumors. *J Med Chem* **2014,** 57, 2413-28.
(18) Liang, Y.; Gao, S.; Wan, H.; Wang, J.; Chen, H.; Zheng, Z.; Hu, X. Syntheses and resolutions of new chiral biphenyl backbones: 2-amino-2′-hydroxy-6,6′-dimethyl-1,1′-biphenyl and 2-amino-2′-hydroxy-4,4′,6,6′-tetramethyl-1,1′-biphenyl. *Tetrahedron: Asymmetry* **2003,** 14, 1267-1273.
(19) Banister, S. D.; Wilkinson, S. M.; Hanani, R.; Reynolds, A. J.; Hibbs, D. E.; Kassiou, M. A practical, multigram synthesis of the 2-(2-(4-alkoxyphenyl)-5,7-dimethylpyrazolo[1,5-a]pyrimidin-3-yl)acetamide (DPA) class of high affinity translocator protein (TSPO) ligands. *Tetrahedron Lett.* **2012,** 53, 3780-3783.
(20) Motulsky, H.; Christopoulos, A. *Fitting models to biological data using linear and nonlinear regression : a practical guide to curve fitting*. Oxford University Press: Oxford ; New York, 2004; p 351 p.
(21) Christopoulos, A.; Kenakin, T. G protein-coupled receptor allosterism and complexing. *Pharmacol Rev* **2002,** 54, 323-74.
(22) Jaremko, L.; Jaremko, M.; Giller, K.; Becker, S.; Zweckstetter, M. Structure of the mitochondrial translocator protein in complex with a diagnostic ligand. *Science* **2014,** 343, 1363-6.
(23) Li, F.; Xia, Y.; Meiler, J.; Ferguson-Miller, S. Characterization and modeling of the oligomeric state and ligand binding behavior of purified translocator protein 18 kDa from Rhodobacter sphaeroides. *Biochemistry* **2013,** 52, 5884-99.
(24) Delavoie, F.; Li, H.; Hardwick, M.; Robert, J. C.; Giatzakis, C.; Peranzi, G.; Yao, Z. X.; Maccario, J.; Lacapere, J. J.; Papadopoulos, V. In vivo and in vitro peripheral-type benzodiazepine receptor polymerization: functional significance in drug ligand and cholesterol binding. *Biochemistry* **2003,** 42, 4506-19.
(25) Sakai, M.; Ferraz-de-Paula, V.; Pinheiro, M. L.; Ribeiro, A.; Quinteiro-Filho, W. M.; Rone, M. B.; Martinez-Arguelles, D. B.; Dagli, M. L.; Papadopoulos, V.; Palermo-Neto, J. Translocator protein (18 kDa) mediates the pro-growth effects of diazepam on Ehrlich tumor cells in vivo. *Eur J Pharmacol* **2010,** 626, 131-8.
(26) Boujrad, N.; Gaillard, J. L.; Garnier, M.; Papadopoulos, V. Acute action of choriogonadotropin on Leydig tumor cells: induction of a higher affinity benzodiazepine-binding site related to steroid biosynthesis. *Endocrinology* **1994,** 135, 1576-83.
(27) Boujrad, N.; Vidic, B.; Papadopoulos, V. Acute action of choriogonadotropin on Leydig tumor cells: changes in the topography of the mitochondrial peripheral-type benzodiazepine receptor. *Endocrinology* **1996,** 137, 5727-30.
(28) Brown, R. C.; Degenhardt, B.; Kotoula, M.; Papadopoulous, V. Location-dependent role of the human glioma cell peripheral-type benzodiazepine receptor in proliferation and steroid biosynthesis. *Cancer Lett* **2000,** 156, 125-32.
(29) Lagoja, I. M.; Pannecouque, C.; Aerschot, A. V.; Wivrouw, M.; Debyser, Z.; Balzarini, J.; Herdewijn, P.; Clercq, E. D. N–Aminoimidazole Derivatives Inhibiting Retroviral Replication via a Yet Unidentified Mode of Action. *J. Med. Chem.* **2003,** 46, 1546–1553.
(30) Heitsch, H.; Becker, H. A.; Kleemann, H.; Wagner, A. *Bioorg Med Chem* **1997,** 5, 673–678.
(31) Yutilov, Y.; Svertilova, L.; Minkina, L.; Kirillova, K.; Smolyar, N. Improvement of the Synthesis of 6–Bromo–5–methylimidazo[4,5–b]pyridine, a Stabilizer for Color Photography. *Russian Journal of Applied Chemistry* **2005,** 78, 787–790.

Tables:

Table 1. Nature of binding interaction and TSPO affinities for compounds **1** – **5**. n_H indicates hill slope value.

		Best–fit binding model		Ki (nM)	
Cpd	**Structure**	**T98G**	**HEK**	**T98G**	**HEK**
1	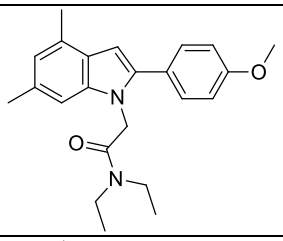	variable slope (n_H: –2.11 ± 0.05)	variable slope (n_H: –1.74 ± 0.38)	806.00 ± 96.77	28.13 ± 8.18
2	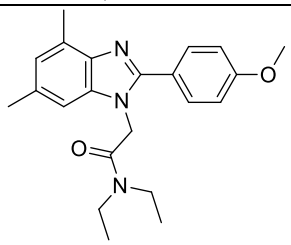	variable slope (n_H: –0.52 ± 0.21)	one–site	398.18 ± 99.99	224.46 ± 131.5
3	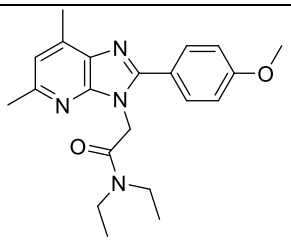	one–site	one–site	144.33 ± 66.79	29.11 ±21.39
4	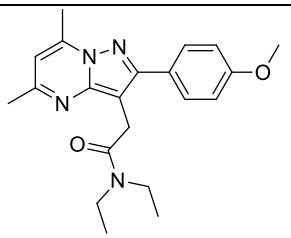	one–site	one–site	6.68 ± 1.45	8.20 ± 2.17
5	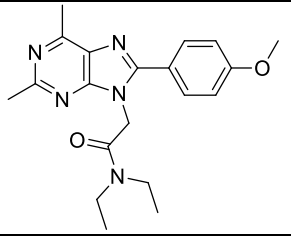	N/A	N/A	> 10 μM	> 10 μM

Figures, schemes/structures and charts:

Scheme 1. Synthetic route to Indole derivative **1**[a]

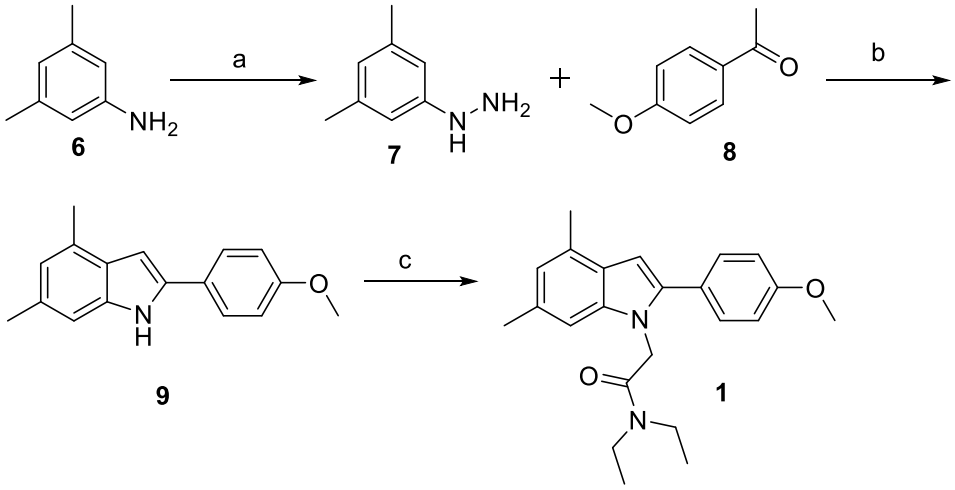

[a]**Reagents and conditions:** (a) 1. Aq $NaNO_2$, conc HCl, –10 °C, 30 min. 2. $SnCl_2$, conc HCl, –5 °C to RT, 30 min. 3. 3M KOH, DCM, 30 min, 40% over three steps; (b) 1. Cat. AcOH, EtOH, reflux, 2 h 2. PPA, 120 °C, 30 min (c) NaH, $ClCH_2CONEt_2$, DMF, 0 °C to RT, overnight, 47%.

Scheme 2. Synthetic route to Benzimidazole derivative **2**[a]

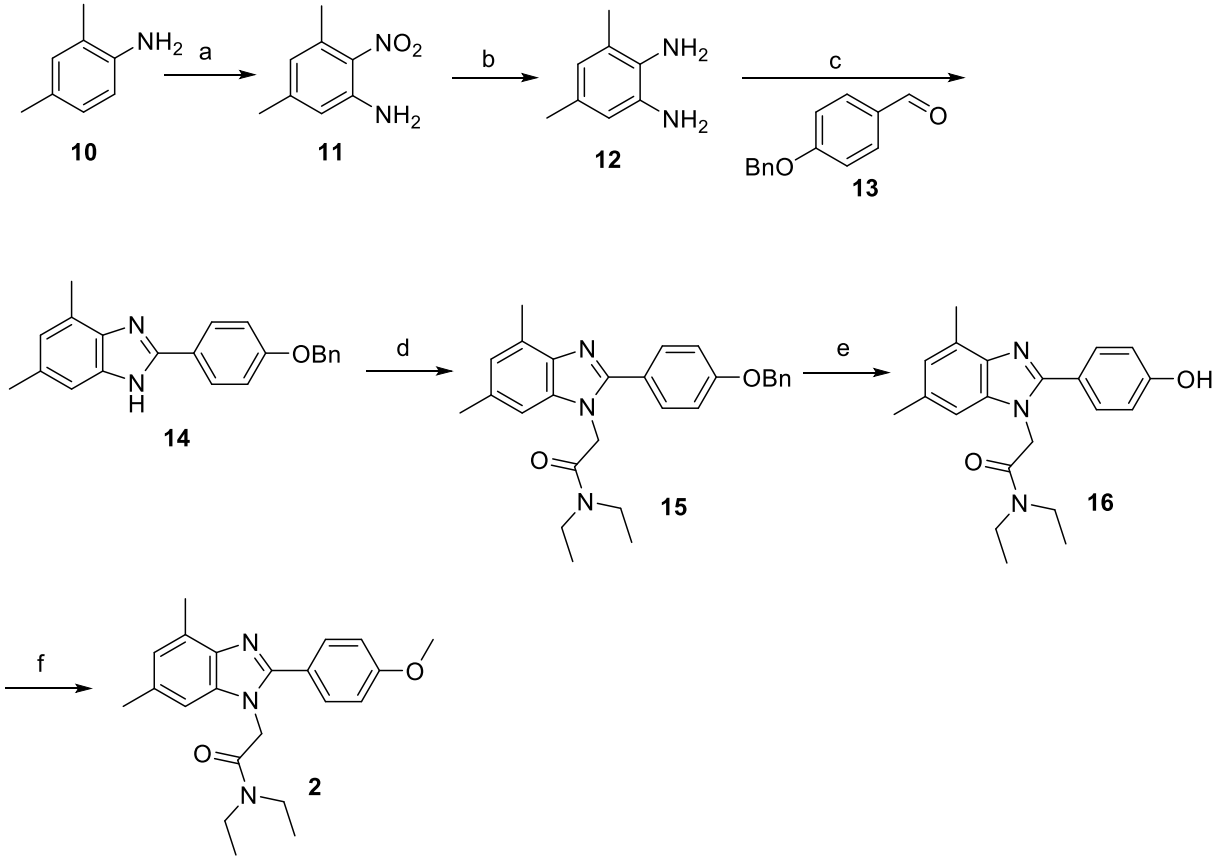

[a]**Reagents and conditions:** (a) i) Ac_2O, Conc. HNO_3, 0 °C, 10 min ii) conc. HCl, ethanol, reflux, overnight, 78% (b) $NH_2NH_2{\cdot}H_2O$, Zn powder, n–butanol, reflux, 6 h, 91%; (e) NH_4OAc, abs. EtOH, MW, 75 °C, 2.5 h, 81%; (f) NaH, $ClCH_2CONEt_2$, DMF, 0 °C to RT, overnight, 70%; (g) H_2, 10 % Pd/C, MeOH, RT, 12 h, 91%; (h) MeI, NaH, DMF, 0 °C to RT, overnight 89%.

Scheme 3. Synthetic route to Imidazopyridine derivative **3**[a]

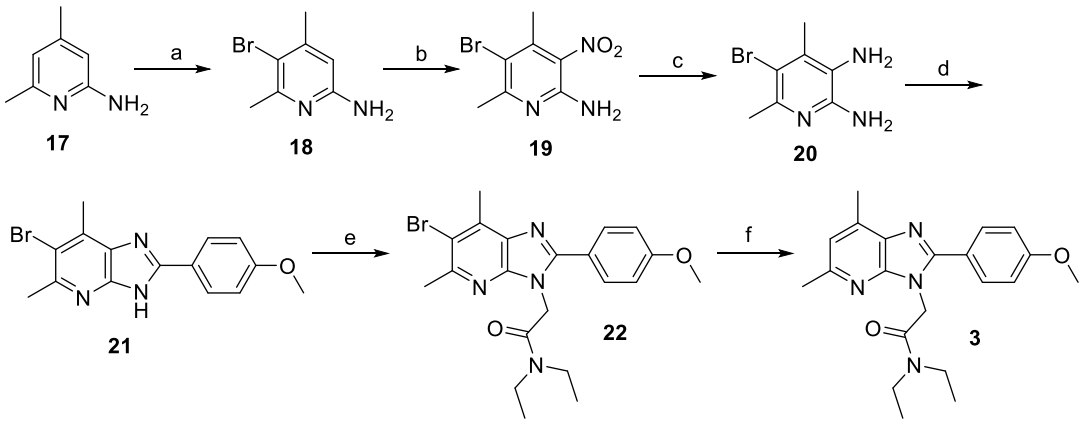

[a]**Reagents and conditions:** (a) 1,3–dibromo–5,5–dimethylimidazolidine–2,4–dione, CH_2Cl_2, – 50 °C, 30 min, 76%; (b) Conc. HNO_3, 6N H_2SO_4, – 10 °C to RT, 30 min, 91%; (c) $NH_2NH_2{\cdot}H_2O$, Zn powder, *n*–BuOH, reflux, overnight, 90%; (d) 4–methoxy benzaldehyde, NH_4OAc, abs. EtOH, 75 °C, MW, 2.5 h, 80%; (e) NaH, $ClCH_2CONEt_2$, DMF, 0 °C to RT, overnight, 75%; (f) n–BuLi, THF, –50 °C, 1 h, 89%.

Scheme 4. Synthetic route to purine derivative **5**[a]

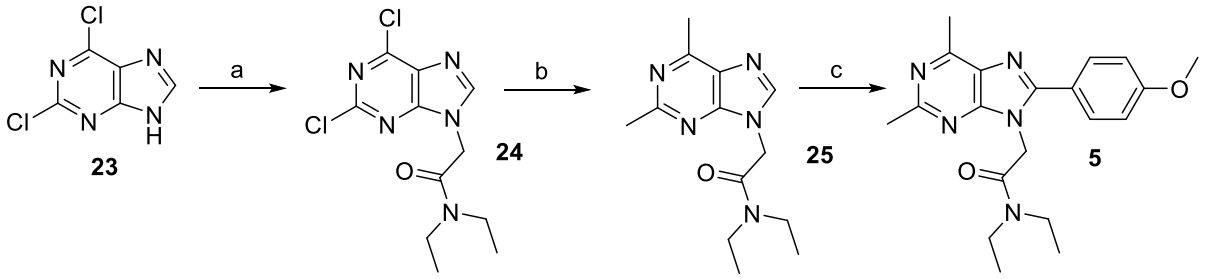

[a]**Reagents and conditions:** (a) K_2CO_3, $ClCH_2CO_2Et$, DMF, 152 °C, MW, 15 min; (b) Me_3Al, $Pd(PPh_3)_4$, THF, reflux, overnight, 45% over two steps; (c) 4–Iodoanisole, $Pd(OAc)_2$, CuI, Cs_2CO_3, DMF, 120 °C, 13 h, 58%.

Figure 1

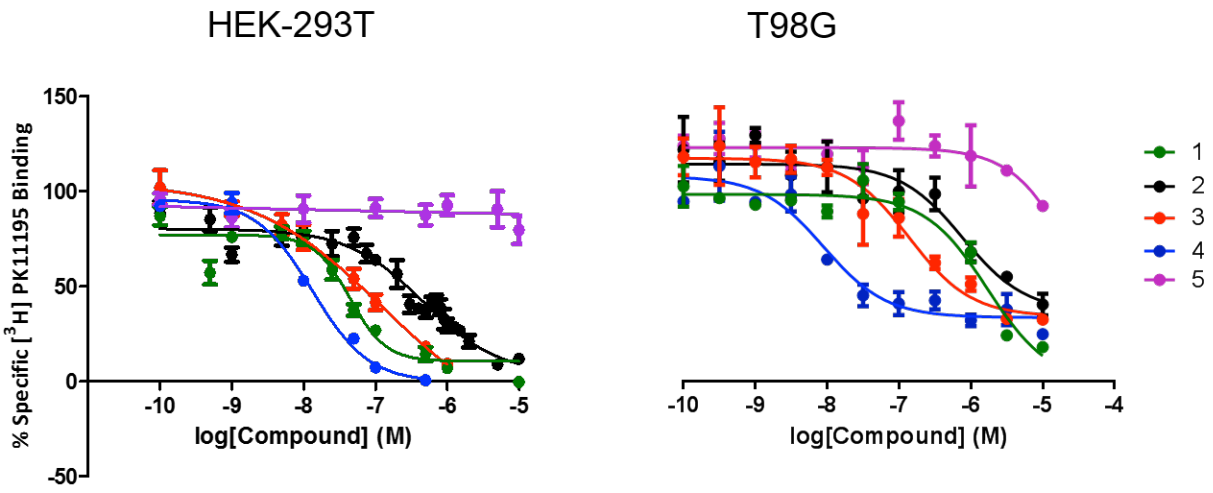
HEK-293T
T98G
% Specific [3H] PK11195 Binding
150
100
50
0
-50
-10
-9
-8
-7
-6
-5
-4
log[Compound] (M)
1
2
3
4
5

Figure 2

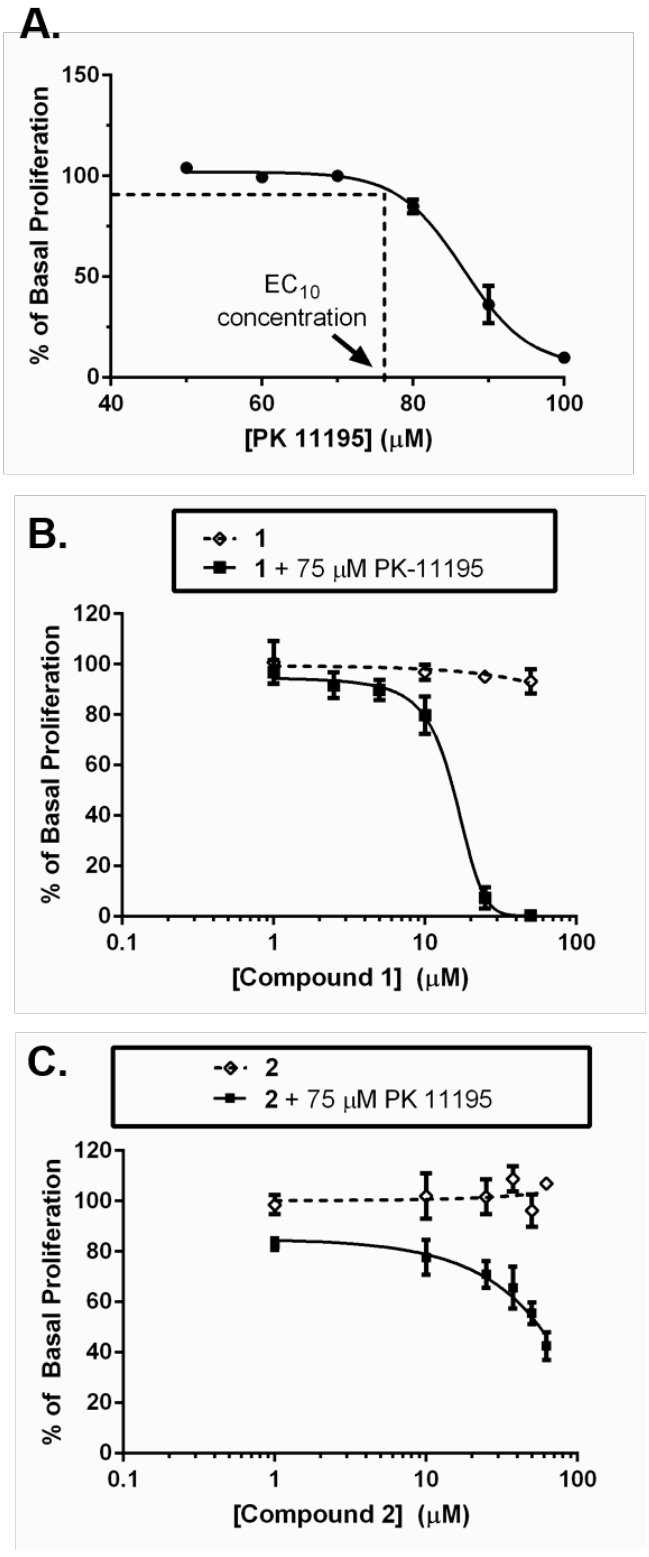
A.
% of Basal Proliferation
150
100
50
0
40
60
80
100
EC10
concentration
[PK 11195] (μM)
B.
1
1 + 75 μM PK-11195
% of Basal Proliferation
120
100
80
60
40
20
0
0.1
1
10
100
[Compound 1] (μM)
C.
2
2 + 75 μM PK 11195
% of Basal Proliferation
120
100
80
60
40
20
0
0.1
1
10
100
[Compound 2] (μM)

Figure legends

Figure 1. The effect of changing the number of nitrogens in the heteratomic core of pyrazolopyrimidine acetamide–derived compounds on competition with [^{3}H] PK 11195 at the human TSPO in HEK–293T cells (left) and T98G cells (right).

Figure 2. Dose-response curve of the anti-proliferative effect of PK 11195 on T98G cells (A). Positive modulation of the anti–proliferative effect of an ~EC_{10} concentration of PK 11195 by **1** (B) and **2** (C) in T98G cells. Values represent mean ± S.D of a representative experiment, repeated in triplicate.